Mining Science, vol. 27, 2020, 283–302

www.miningscience.pwr.edu.pl

Mining Science

(Previously Prace Naukowe Instytutu Gornictwa Politechniki Wroclawskiej, ISSN 0370-0798)

ISSN 2300-9586 (print)
ISSN 2353-5423 (online)

Received December 20, 2019; Reviewed; Accepted September 25, 2020

ANALYZING METHOD TO EVALUATE EFFECT OF ROADWAY PRESSURE RELIEF

Lei FAN, Weijun WANG*,
Chao YUAN

School of Resources, Environment, and Safety Engineering, Hunan University of Science and Technology, Xiangtan, Hunan 411201, China

Abstract: Based on the theory of matter–element extension, this paper uses the calculation results of FLAC 3D (Fast Lagrangian Analysis of Continua) as raw data to systematically evaluate the effects of roadway pressure relief under different pressure relief options. The results show that: 1) Pressure relief can reduce rock stress on the mining roadway to a certain extent by arranging the pressure relief roadway above or on one side of it. However, the low-stress area formed by the former is larger than that created by the latter. Moreover, appropriately increasing the width of the pressure relief roadway above the mining roadway can effectively improve the stress environment of the mining roadway. 2) The excavation sequence of the pressure relief roadway and the mining roadway has a greater impact on the pressure relief effect. Adopting the method of "excavating the pressure relief roadway first, and after the stress of the surrounding rock of the pressure relief roadway is stabilized, then excavating the mining roadway" can greatly reduce or avoid the disturbance effect caused by the pressure relief roadway excavation. This sequence of excavation can significantly reduce or avoid the effects of disturbances caused by the excavation of the pressure relief roadway. 3) Excavating the pressure relief roadway on one side of the mining roadway can effectively reduce the deformation of its roof, and arranging the pressure relief roadway above the mining roadway can effectively control the deformation of its two sides. Appropriately increasing the width of the pressure relief roadway above the mining roadway can improve the effect of pressure relief.

***Keywords*:** *matter–element extension; roadway pressure relief; effect evaluation; method of analysis*

* Corresponding author: wjwang@hnust.edu.cn (W.J. Wang)

doi: 10.37190/msc202719

1. INTRODUCTION

With advances in coal mining, the environment for resource extraction is becoming more complex, and drastically increases the difficulty of mining. The strong ground pressure encountered in deep resource exploitation poses daunting challenges for roadway support. Reducing rock stress on the roadway, improving the effects of support and the production environment of underground resources have emerged as important subjects for scholars at home and abroad. Roadway pressure relief has become a necessary measure to control the rock surrounding the roadway. By excavating the pressure relief roadway, rock stress in the mining area can be redistributed so that the mining roadway is in an area of reduced stress to achieve the purpose of roadway pressure relief. This helps reduce damage owing to high underground stress in coal mining and ensure the safety of personnel (Qian et al. 2003). Researchers have reported outstanding results in controlling rock surrounding roadways. Based on Kastner's theory, Wang et al. (2016) found that large deformation in deep roadways originate from the continuous deformation of the surrounding rock and the discontinuous deformation of broken surrounding rock around the roadways. Ma et al. (2015) studied the mechanism of the formation of the plastic zone of the rock surrounding a deep-mining roadway, and found that it exhibited three distribution patterns: circular, elliptical, and butterfly. Hou (2017) studied the mechanical characteristics of the rock (coal) roadway in a deep and complex environment, and found that floor heaving and creeping large deformations were the main difficulties in supporting rock surrounding the roadway. They proposed improving the stability of the surrounding rock by reinforcing the floor and corners and using appropriate support methods. Zhao et al. (2016) used plastic zone theory to study the roof control technology for large deformations in mining roadways, and found that rock breaks in the top leaves of butterfly-type roof control technology increases the burden on the anchor (cable) support system. They proposed replacing the ordinary bolts (cables) with the long anchor rod as a butterfly-type roof top control technology. Li et al. (2018) studied the variation in the principal stress field of the lateral surrounding rock of a goaf through theoretical analysis and a field test, and proposed deep control technology along the empty roadway. The basis for the design basis and the replacement of the ordinary anchor cable with the long bolt can yield better engineering results. Based on engineering practice, Mo et al. (2019) studied the management technology of roadway floors and found that high horizontal stresses with greater depths of cover and certain types of floor lithology configuration were mainly likely to contribute to failures of floor strata. Wang et al. (2019) used similar simulation experiments as research methods to study the mechanical characteristics of top coal in the extra-thick coal seam mining project as well as the coordination relationship between top coal and the support. They proposed fully mechanized caving mining technology for extra-thick coal seams for safe mining. Li et al. (2018) used the RFPA (Realistic Failure Process Analysis) to carry out pressure relief simulation

experiments in a mining roadway with high stress and large deformation, found that through the excavation pressure relief roadway, when a pressure relief lane and coal pillar spacing of 15 m were maintained, the effect of roadway pressure relief was more prominent. The maximum pressure of the coal pillar was reduced by 22.6%, and rock stress of the roadway was significantly reduced. Ma et al. (2019) studied the mechanical properties of the overlying strata after the top-loading of the Tashan coal mine. Based on the mechanical model of the channel in different surrounding rock structures, measures for roadway control were studied and proposed. Based on a numerical simulation, Han et al. (2017) proposed and analyzed the roof control method of "pressure relief anchor" dual-active control, and achieved good test results using engineering practice. Zuo et al. (2019) revealed the mechanical mechanism of the unloading of the groove and claimed that the deformation in the deep roadway with the soft rock can be effectively controlled by opening and unloading the groove. Zhu et al. (2015) studied the influence of the depth of the pressure-relieving groove on the effect of pressure relief by RFPA, and found that this effect was apparent at depth equal to the radius of the roadway.

The above research focused on studying the deformation in, and the failure characteristics and laws of rocks surrounding roadways. Only by analyzing comparative experimental results under various factors can a comprehensive evaluation of the effects of the surrounding rock control technology be conducted. Based on past research, the authors of this paper combine extension theory with rock control technology for the roadway, select the position and shape of the pressure relief roadway as the main variable, and establish an evaluation index for rock control technology. Through theoretical calculations and analysis of numerical simulations, the effects of pressure relief under different pressure relief schemes are systematically evaluated to determine the optimal scheme by selecting the location and size of the pressure relief roadway as primary variables.

2. BASIC EXTENSION THEORY

Extenics has penetrated into many aspects of the mining field. Evaluations of mine safety, stability of the slope of the mine, and the stability of rock surrounding the mine using the theory of extenics have become important for scientific mining (Xu et al. 2018). Using matter–element extension analysis, qualitative and quantitative methods are combined to form a systematic, scientific, and practical method to assess the effect of pressure relief on rock surrounding the roadway. Theoretical reference is made to guide scientific mining and optimize options for roadway pressure.

Extenics consists of an ordered collection of objects N, features C, and feature values V to be evaluated, and are denoted by R = (objects, characteristics, magnitude) = (N, C, V). This collection is called the matter element of the object to be evaluated.

$R_j = (N, C_j, V_j)$ (j = 1, 2, ..., n) is a discrete element, C_j (j = 1, 2,·..., n) is the evaluation feature, V_j (j = 1, 2,·..., n) is the evaluation value corresponding to each evaluation feature, and the specific matter element is expressed as follows:

$$\mathbf{R} = \begin{bmatrix} R_1 \\ R_2 \\ R_3 \\ R_4 \end{bmatrix} = \begin{bmatrix} N & C_1 & V_1 \\ & C_2 & V_2 \\ & \vdots & \vdots \\ & C_n & V_n \end{bmatrix}. \tag{1}$$

3. ANALYTIC HIERARCHY PROCESS TO ESTABLISH EVALUATION MODEL

As shown in Fig. 1, the evaluation index is established by using the analytic hierarchy process (AHP). We first calculate the judgment matrix **B** and obtain the weight of each index, and then calculate the maximum eigenvalue $\lambda_{\max}$ of the judgment matrix. Finally, the size of C_R is tested by $C_R = \dfrac{C_I}{R_I}$, and the consistency check of matrix **B** is performed (Guo et al. 2017). Thus, the index weights of each evaluation index are obtained in order of W_1, W_2, ..., W_n.

Matrix

$$\mathbf{B} = \begin{bmatrix} b_{11} & b_{12} & \ldots & b_{1n} \\ b_{21} & b_{22} & \ldots & b_{2n} \\ \vdots & \vdots & & \\ b_{n1} & b_{n1} & \ldots & b_{nm} \end{bmatrix}, \quad C_I = \frac{\lambda_{\max} - 1}{n - 1}.$$

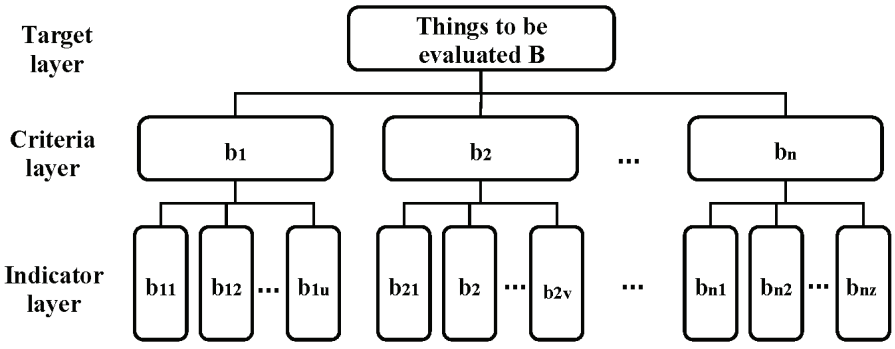

Fig. 1. AHP analysis indicator system

3.1. EVALUATING EXTENSION THEORY

3.1.1. THE DETERMINATION OF THE CLASSICAL DOMAIN

$$\mathbf{R}_{0t} = [N, C_j, V_{0tj}] = \begin{bmatrix} N & C_1 & \langle a_{0t1}, b_{0t1} \rangle \\ & C_2 & \langle a_{0t2}, b_{0t2} \rangle \\ & \vdots & \vdots \\ & C_n & \langle a_{0tn}, b_{0tm} \rangle \end{bmatrix}, \tag{2}$$

In the above, $\mathbf{R}_{0t}$ is the matter element of the classical domain; c_j (j = 1,2, ..., n) is the j-th evaluation index of the object to be evaluated; and V_{tj} (j = 1,2, ..., n) is the range of magnitude of the j-th evaluation index in the t-th evaluation category (t = 1, 2, ..., k, $V_{0tj} = \langle a_{0tj}, b_{0tj} \rangle$).

3.1.2. THE DETERMINATION OF THE SECTION

$$\mathbf{R}_p = [N, C_j, V_p] = \begin{bmatrix} N & C_1 & \langle a_{p1}, b_{p1} \rangle \\ & C_2 & \langle a_{p2}, b_{p2} \rangle \\ & \vdots & \vdots \\ & C_n & \langle a_{pn}, b_{pn} \rangle \end{bmatrix}, \tag{3}$$

where: $\mathbf{R}_p$ is the matter element of domain; C_j (j = 1, 2, ..., n) is the j-th evaluation index of the object to be evaluated; and V_{pj} (j = 1, 2,·..., n) is the range of magnitudes taken for the j-th evaluation index C_j (j = 1, 2,·..., n) of the object to be evaluated, V_{pj} (j = 1, 2,·..., n).

3.1.3. THE DETERMINATION OF THE OBJECT TO BE EVALUATED

$$\mathbf{R}_{ij} = [N_i, C_j, V_{ij}] = \begin{bmatrix} N_i & C_1 & V_{i1} \\ & C_2 & V_{i2} \\ & \vdots & \vdots \\ & C_n & V_{in} \end{bmatrix}, \tag{4}$$

$\mathbf{R}_{ij}$ is the object to be evaluated (i = 1, 2, ..., m; j = 1, 2, ..., n). The evaluation index C_j (j = 1, 2,·..., n) of $\mathbf{R}_{ij}$ is scored, and the obtained value (the actual score) is recorded as V_{ij}.

3.1.4. CALCULATION OF CORRELATION

The j-th index C_j (j = 1, 2,·..., n) of the thing to be evaluated N_i (i = 1, 2,·..., m) is about the evaluation level t (t = 1, 2, ..., g). The relational degree function expression is:

$$k_t(V_{ij}) = \begin{cases} \dfrac{\rho[V_{ij}(t), V_{0tj}]}{\rho[V_{ij}(t), V_{pj}] - \rho[V_{ij}(t), V_{0tj}]}, \rho[V_{ij}(t), V_{pj}] \neq \rho[V_{ij}(t), V_{0tj}] \\ -\rho[V_{ij}(t), V_{0tj}] - 1, \rho[V_{ij}(t), V_{pj}] = \rho[V_{ij}(t), V_{0tj}] \end{cases} \tag{5}$$

$$\begin{cases} \rho[V_{ij}(t), V_{0tj}] = \left| V_{ij} - \dfrac{1}{2}(b_{0tj} + a_{0tj}) \right| - \dfrac{1}{2}(b_{pj} - a_{pj}) \\ \rho[V_{ij}(t), V_{pj}] = \left| V_{ij} - \dfrac{1}{2}(b_{pj} + a_{pj}) \right| - \dfrac{1}{2}(b_{pj} - a_{pj}) \end{cases} \tag{6}$$

3.1.5. THE DETERMINATION OF THE RATING

Record all the calculated correlation degrees in matrix form, so the correlation degree matrix **K** is:

$$\mathbf{K} = \begin{bmatrix} k_{11} & k_{21} & \ldots & k_{g1} \\ k_{12} & k_{22} & \ldots & k_{g2} \\ \vdots & \vdots & & \vdots \\ k_{1n} & k_{2n} & \ldots & k_{gn} \end{bmatrix} \tag{7}$$

$$\mathbf{Y}(N) = \mathbf{WK} = (W_1, W_2, ..., W_n) \begin{bmatrix} k_{11} & k_{21} & \ldots & k_{g1} \\ k_{12} & k_{22} & \ldots & k_{g2} \\ \vdots & \vdots & & \vdots \\ k_{1n} & k_{2n} & \ldots & k_{gn} \end{bmatrix} = (Y_1, Y_2, ..., Y_g) \tag{8}$$

The maximum value method is used to determine the evaluation level, that is, if $\max(\mathbf{Y}) = Y_t$, the evaluation level of the object to be evaluated N_i is t.

4. MATHEMATICAL SIMULATION

4.1. THE SELECTION OF THE EVALUATION INDICATORS

The selection of the evaluation indicators plays an important role in the assessment of the effect of pressure relief with different options for it, which is directly related to the final result of the evaluation. The indicators should follow the principles of science, comprehensiveness, and functionality. They should be as simple and effective as possible for a comprehensive evaluation (Han et al. 2018). Based on the mechanical characteristics of the rock surrounding the mine roadway, this paper draws on past re-

search results to formulate the evaluation index system for the effect of relieving pressure on rock surrounding the roadway. There are four first-level indicators: the rate of change in roof subsidence (B_1); rate of change in floor heave (B_2), rate of change in the internal left turn (B_3), and that in the internal right turn (B_4), as shown in Table 1.

1) The rate of change in roof subsidence. This rate of change is the percentage of the difference between the absolute values of roof subsidence before and after pressure relief and roof subsidence without pressure relief. It indicates the degree of deformation and breakage of the roof of the roadway under stress from the surrounding rock of the deep roadway. The smaller the rate of change, the worse the effect of roadway pressure relief on the roof.
2) The rate of change in floor heave. When pressure on the roadway due to the surrounding rock is too large, the floor bulges into the roadway, causing problems for underground traffic. The larger the value of the index is, the smaller is floor heave after pressure relief, and the better is the effect of pressure relief on the floor.
3) The rate of change in the internal shift of light hand (right hand). This refers to the percentage of change in light-hand (right-hand) deformation before and after pressure relief, and the magnitude of displacement of the light hand (right hand) before pressure relief. It reflects the effect of the pressure relief option at two sides of the roadway. The larger the value of the index is, the better is the effect of pressure relief on the roadway.

4.2. DETERMINING INDICATOR WEIGHTS

The weights of the roadway pressure relief evaluation index reflect the importance of each object to the evaluation results. This paper applies the AHP to obtain the weights of the relevant indicators to assess the effect of pressure relief on the roadway. In determining weights of the index, based on the control theory of the roadway, the results of past research are used (Qian et al. 2003; Gou et al. 2003; Zhang et al. 2010; Zhang et al. 2016). An index weight was objectively and independently scored by multiple (>5) experts or scholars, and the weights of the roadway pressure relief effect evaluation index were then obtained. The process is omitted here (see Table 1 for details).

Table 1. Weights of roadway pressure relief evaluation index

Target layer	Evaluation index	Index weight	Result parameter
Evaluation of pressure relief effect of roadway surrounding rock	The rate of change in roof subsidence (B_1)	0.436	$C_I = 0.003$ $R_I = 0.900$ $C_R = 0.003$
	The rate of change in floor heave (B_2)	0.252	
	The rate of change in the internal shift of light hand (B_3)	0.156	
	The rate of change in the internal shift of right hand (B_4)	0.156	

4.3. DETERMINING LEVEL OF EVALUATION

The determination of the level of evaluation of the matter–element extension provides an important reference for the evaluation results (Li et al. 2015). Based on the overview of a project, this paper divided the evaluation results into five evaluation grades. According to the effect of pressure relief on the roadway, the grades were I, II, III, IV, and V. The meaning and range of each grade are shown in Table 2.

Table 2. Range of values of evaluation level indicators

Evaluation level	I	II	III	IV	V
	Very poor pressure relief	Poor pressure relief	Pressure relief effect is general	Better pressure relief	Good pressure relief
The rate of change in roof subsidence (B_1)	[–10, 2)	[2, 14)	[14, 26)	[26, 38)	[38, 50)
The rate of change in floor heave (B_2)	[–10, 2)	[2, 14)	[14, 26)	[26, 38)	[38, 50)
The rate of change in the internal shift of light hand (B_3)	[–10, 2)	[2, 14)	[14, 26)	[26, 38)	[38, 50)
The rate of change in the internal shift of right hand (B_4)	[–10, 2)	[2, 14)	[14, 26)	[26, 38)	[38, 50)

5. ENGINEERING APPLICATIONS

5.1. BACKGROUND OF APPLICATION

The model was calculated using the FLAC 3D numerical simulation software, and a 3D model with dimensions of 100 m × 100 m × 100 m (width × height × deep) was simulated. The center of the model was a rectangular roadway with a size of 6 m × 4 m (width × height). The roadway was surrounded by free boundaries, indicating that it was not supported after excavation. Local mesh encryption was performed near the roadway in the center of the model. The total number of grids in the model was 278 861.

The model used the Mohr–Coulomb constitutive model and consisted of four layers, which in turn represented sandstone 1, fine sandstone, shale, and sandstone 2. The model parameters are shown in Table 3. The left and right boundaries of the model were fixed with normal displacement, the bottom was fixed, and the top was free.

To obtain simulation result close to the situation on the ground, 3D directional stresses were applied inside the model to simulate the original stress of the rock mass: horizontal stress s_{xx} = 9 MPa, vertical stress s_{zz} = 28 MPa, and intermediate

stress s_{yy} = 11 MPa. At the initial equilibrium, the tensile strength and cohesion of the model were increased to avoid plastic damage. Once the initial geostress field had formed, the displacement and plastic zone generated by the first equilibrium were cleared, and the model parameters were assigned to perform the balance calculation.

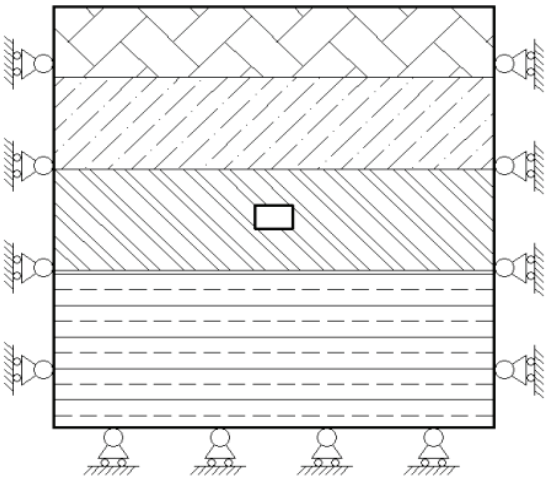

Fig. 2. Schematic diagram of the numerical simulation model

Table 3. Basic parameters of numerical simulation

Name	Unit	Sandstone 1	Fine sandstone	Shale	Sandstone 2
Bulk modulus K	GPa	1.2	2.8	0.27	3.3
Shear modulus G	GPa	0.82	0.97	0.064	0.5
Tensile strength τ	MPa	1.25	0.83	0.046	0.35
Density ρ	kg/m^3	2350	2470	2135	2320
Internal friction angle φ	°	34	36	30	37
Cohesion C	MPa	0.96	2.3	0.04	1.0

To accurately simulate the geological environment of the roadway, the initial calculation of the balance of the model was based on the basic mechanical parameters of the rock mass. The displacement, velocity, and plastic zone of the surrounding rock generated by the initial equilibrium were calculated, and the initial original rock stress field was obtained. Then, the excavated mining roadway, and the redistribution of the stress and displacement fields of rock surrounding the roadway were determined, and the displacement cloud map and stress cloud diagram of the sur-

rounding rock after the excavation of the mining roadway were calculated, as shown in Figs. 3 and 4.

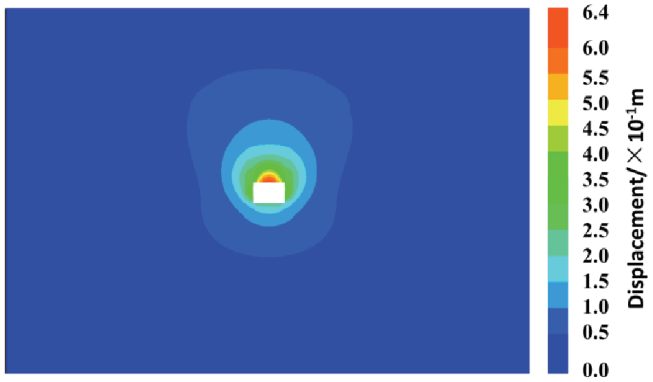

Fig. 3. Map of displacement cloud after roadway excavation

Fig. 4. Stress cloud after roadway excavation

5.2. OVERVIEW OF PRESSURE RELIEF OPTIONS

1) Selecting position of pressure relief roadway. The selection of the location of the pressure relief roadway directly affects the final effect of pressure relief (Yu et al. 2016). When the pressure relief roadway was too close to the mining roadway, the protection coal pillar between the roadways was severely deformed and even collapsed. This increases the risk of accidents in the mining roadway. When the pressure relief roadway was too far from the mining roadway, changes in the stress of the surrounding rock caused by the pressure relief roadway had little or no effect on the mining roadway, and the effect of pressure

relief was poor. In this paper, by referring to the results of previous research, a FLAC 3D numerical simulation was used for calculation, and the distance between the pressure relief roadway and the mining roadway was determined to be 6 m at the bottom of the mining roadway.

2) Determining excavation sequence of the roadway. The excavation of the pressure relief roadway and mining roadway has a significant influence on the effect of pressure relief (Wang et al. 2017), There are usually two excavation sequences to choose from: excavating the mining roadway and then excavating the pressure relief roadway, or vice versa. This excavation method has strong engineering flexibility. The option for pressure relief does not need to be formulated before roadway excavation. It can be temporarily determined according to the needs of mining engineering. However, due to the excavation of the pressure relief roadway, the mining roadway, and the formation, disturbance in the surrounding rock was very large, and could easily cause secondary damage to the mining roadway.

The pressure relief roadway was first excavated, and the mining roadway was then re-excavated after stress in the surrounding rock stress had been redistributed. This method can avoid the effect of disturbance in the excavation pressure relief roadway on the mining roadway. Below is the displacement diagram of the roof and the floor under the excavation sequences of two pressure relief roadways in options 1 and 3.

Through comparative analysis, the sequence of the excavation of the pressure relief roadway followed by that of the mining roadway was more reasonable.

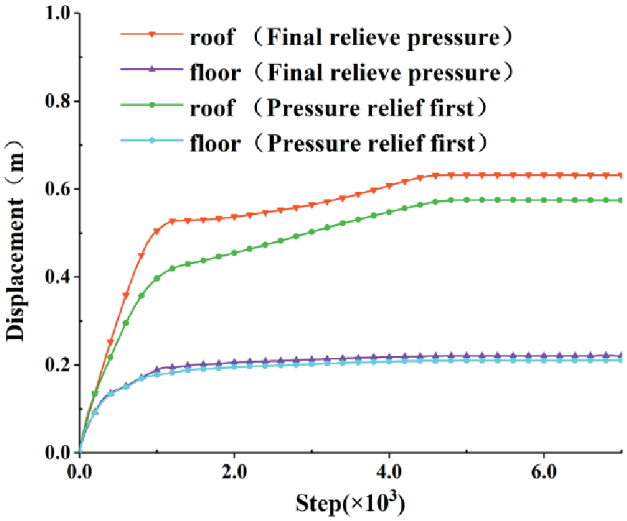

Fig. 5. Displacement of roof and floor in option 1
under different tunnel excavation sequences

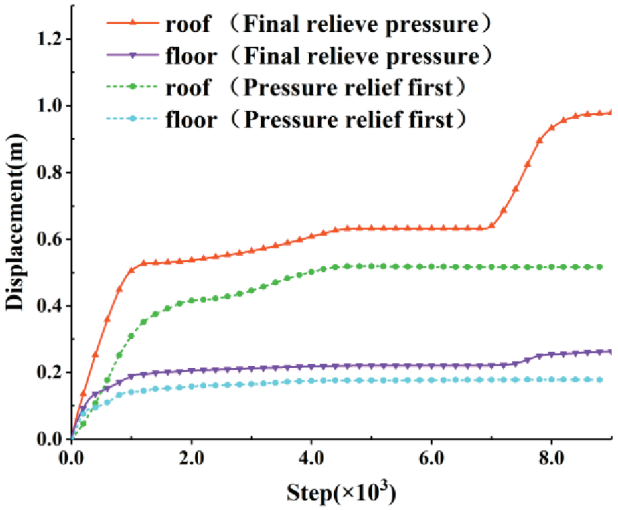

Fig. 6. Displacement of roof and floor in option 3 under different tunnel excavation sequences

3) Determining option for pressure relief roadway. According to the situation of a project, four pressure relief options were selected for comparative study. The specific options are as follows:

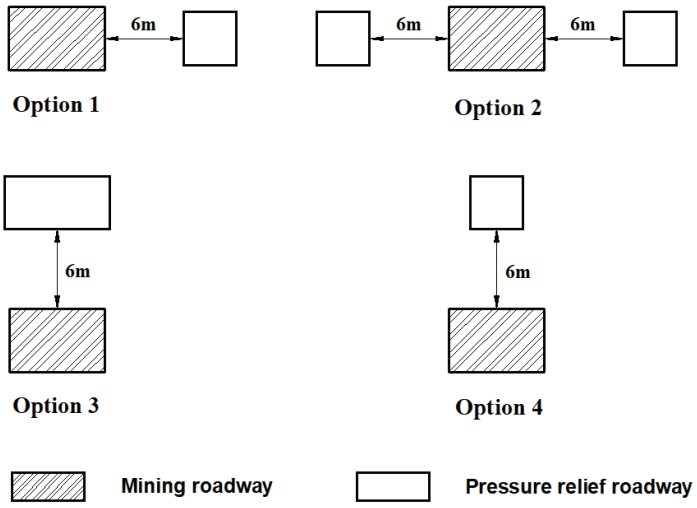

Fig. 7. Schematic diagram of pressure relief options

Option 1: It arranged a pressure relief roadway 6 m from the right side of the mining roadway, and the size of the pressure relief roadway was 4 m × 4 m (width × height).

Option 2: It arranged two pressure relief roadways, each of which was 6 m from the left and right sides of the mining roadway, with a size of 4 m × 4 m.

Option 3: It arranged a pressure relief roadway 6 m away from the roof of the mining roadway, and the size of the pressure relief roadway was 8 m × 4 m (width × height).

Option 4: It arranged a pressure relief roadway 6 m from the roof of the roadway, and the size of the pressure relief roadway was 4 m × 4 m (width × height).

6. RESULTS

Numerical calculations of the four pressure relief options were carried out, changes to the stress and displacement of the mining roadway were recorded, and the original data of the numerical simulation were obtained.

6.1. STRESS DISTRIBUTION OF SURROUNDING ROCK

Figures 8–11 show a nephogram of stress distribution in the surrounding roadway after the four pressure relief options had been implemented. After the excavation of the pressure relief roadway, the pattern of stress distribution of the mining roadway changed.

Comparing Fig. 8 with Fig. 9, the principal stress of surrounding rock near the mining roadway (0–3 m) featured a small difference between the options 1 and 2. In addition, when the pressure relief roadway is arranged on both sides of the mining roadway, the low-stress area at the roof was much larger than on the two sides of the roadway.

Comparing Fig. 4, Fig. 8, and Fig. 11, it is clear that the arrangement of the roadway above the roof or on both sides reduced stress due to rock surrounding the mining roadway. However, the low-pressure area formed by placing the pressure relief roadway above the mining roadway was larger than that of the pressure relief roadway disposed on both sides of the mining roadway.

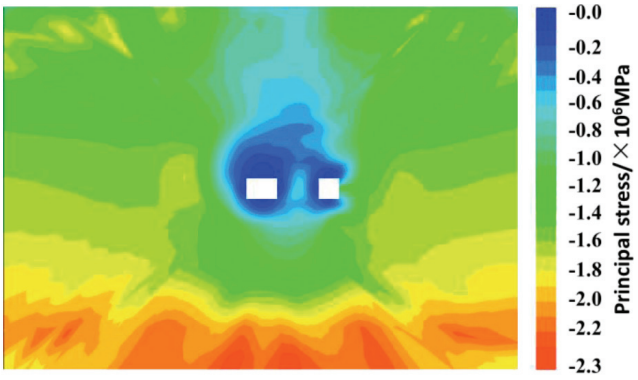

Fig. 8. Stress distribution of the surrounding rock in option 1

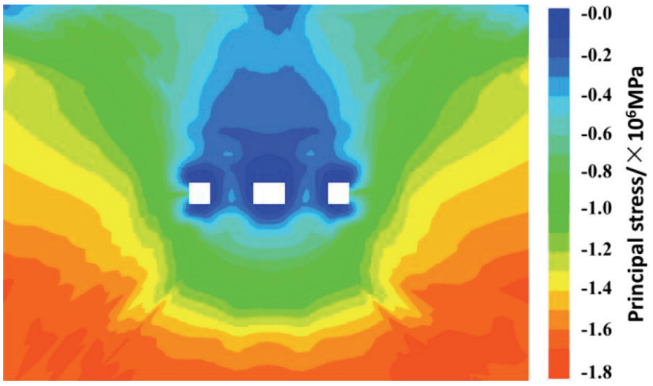

Fig. 9. Stress distribution of the surrounding rock in option 2

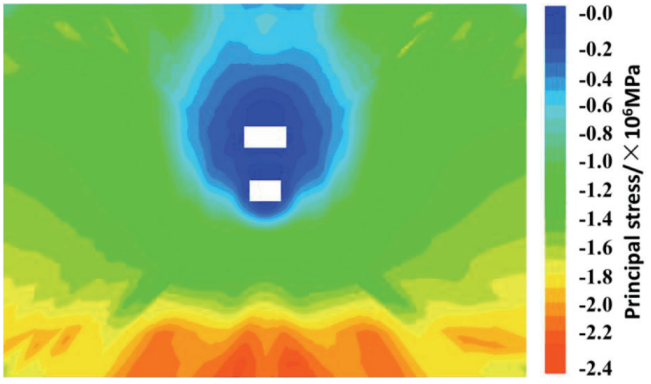

Fig. 10. Stress distribution of the surrounding rock in option 3

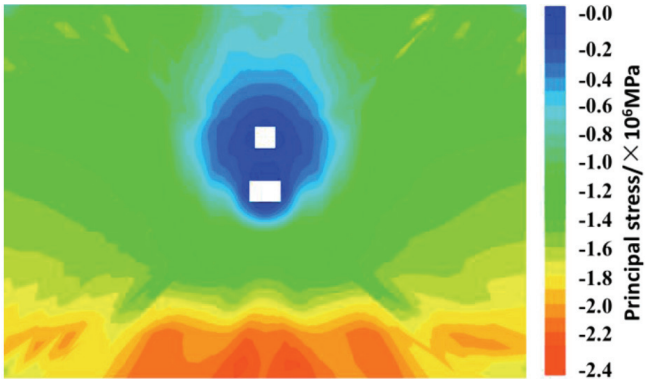

Fig. 11. Stress distribution of the surrounding rock in option 4

Comparing Fig. 10 with Fig. 11, it is evident that increasing the width of the pressure relief roadway above the roof plate within a certain range can effectively reduce stress due to rock surrounding the mining roadway.

6.2. DISPLACEMENT DISTRIBUTION OF SURROUNDING ROCK

Table 4. Raw data for numerical simulation of roadway pressure relief

Evaluation index	No pressure relief	Option 1	Option 2	Option 3	Option 4
Roof subsidence, m	0.6375	0.5745	0.5100	0.5169	0.6469
Floor heave, m	0.2207	0.2108	0.1952	0.1782	0.2043
The internal shift of light hand, m	0.3891	0.4136	0.3738	0.2927	0.3387
The internal shift of light hand, m	0.3892	0.3576	0.3751	0.2943	0.3395
The rate of change in roof subsidence, %	–	10.97	25.00	23.33	–1.45
The rate of change in floor heave, %	–	4.70	13.06	23.85	8.03
The rate of change in the internal shift of light hand, %	–	–5.92	4.09	32.93	14.88
The rate of change in the internal shift of right hand, %	–	8.84	3.76	32.25	14.64

1) Initial evaluation. According to the formulas (1)–(5), the degree of relevance of each evaluation index to the evaluation level was calculated, and the level of extenics evaluation of each of the four pressure relief options was obtained.

Table 5. Evaluation results of each evaluation index for the four pressure relief options

		Relevant evaluation index					Evaluation level
		I	II	III	IV	V	
1	**2**	**3**	**4**	**5**	**6**	**7**	**8**
Option 1	The rate of change in roof subsidence, %	–0.2995	0.2528	–0.1264	–0.4176	–0.5632	II
	The rate of change in floor heave, %	–0.1550	0.2247	–0.3877	–0.5918	–0.6938	II
	The rate of change in the internal shift of light hand, %	0.3397	–0.6603	–0.8301	–0.8868	–0.9151	I

1	2	3	4	5	6	7	8
Option 1	The rate of change in the internal shift of right hand, %	–0.2663	0.4303	–0.2151	–0.4768	–0.6076	II
Option 2	The rate of change in roof subsidence, %	–0.4792	–0.3056	0.0833	–0.0385	–0.3421	III
	The rate of change in floor heave, %	–0.3242	0.0780	–0.0390	–0.3593	–0.5195	II
	The rate of change in the internal shift of light hand, %	–0.1293	0.1744	–0.4128	–0.6085	–0.7064	II
	The rate of change in the internal shift of right hand, %	–0.1134	0.1466	–0.4267	–0.6178	–0.7134	II
Option 3	The rate of change in roof subsidence, %	–0.4444	–0.2592	0.2224	–0.0910	–0.3549	III
	The rate of change in floor heave, %	–0.4552	–0.2736	0.1792	–0.0760	–0.3511	III
	The rate of change in the internal shift of light hand, %	–0.6445	–0.5260	–0.2889	0.4221	–0.2289	IV
	The rate of change in the internal shift of right hand, %	–0.6301	–0.5068	–0.2603	0.4795	–0.2448	IV
Option 4	The rate of change in roof subsidence, %	0.2878	–0.2878	–0.6439	–0.7626	–0.8219	I
	The rate of change in floor heave, %	–0.2506	0.4977	–0.2489	–0.4992	–0.6244	II
	The rate of change in the internal shift of light hand, %	–0.3411	–0.0342	0.0734	–0.3089	–0.4817	III
	The rate of change in the internal shift of right hand, %	–0.3390	–0.0253	0.0533	–0.3156	–0.4867	III

2) Program evaluation. The final evaluation matrix (1 × 5) was obtained by multiplying the evaluation index matrix (1 × 4) of the corresponding option and each evaluation index by an evaluation-level correlation matrix (4 × 5). Using data of option 1 as an example, the calculation is as follows:

$$K(N_1) = [0.436 \quad 0.252 \quad 0.156 \quad 0.156]$$

$$\times \begin{bmatrix} -0.2995 & 0.2528 & -0.1264 & -0.4176 & -0.5632 \\ -0.1550 & 0.2247 & -0.3877 & -0.5918 & -0.6938 \\ 0.3397 & -0.6603 & -0.8301 & -0.8868 & -0.9151 \\ -0.2663 & -0.4303 & -0.2151 & -0.4768 & -0.6076 \end{bmatrix}$$

$$= [-0.1582 \;\; 01.310 \;\; -0.3159 \;\; -0.5439 \;\; -0.6579].$$

Therefore, the pressure relief option 1 had an evaluation grade of II in the assessment of effect of the pressure relief. The effect was poor, and needed to be improved. Similarly, according to the method above, the evaluation results of options 2, 3, and 4 are shown in Table 6.

Table 6. Evaluation results of pressure relief options

Option	Evaluation-level relevance of each program					Evaluation level
	I	II	III	IV	V	
Option 1	–0.1582	0.1310	–0.3159	–0.5439	–0.6579	II
Option 2	–0.3285	–0.0635	–0.1045	–0.2986	–0.5016	II
Option 3	–0.5073	–0.3431	0.0564	0.0818	–0.3171	IV
Option 4	–0.0438	–0.0093	–0.3237	–0.5557	–0.6668	II

7. DISCUSSION

In the engineering example of this paper, based on the proposed evaluation model, the final evaluation grades of the four options were II, II, IV, and II. Therefore, option 3 was the optimal pressure relief solution for this project. By arranging the pressure relief roadway above the mining roadway, roadway pressure relief could be performed more effectively. In option 3, a pressure relief roadway with a size of 8 m × 4 m was arranged 6 m from the roof of the roadway directly above the mining roadway. Once the pressure relief roadway had formed, changes of stress in the surrounding around the roadway stabilized, and the mining roadway was then excavated for recovery. Compared with direct recovery without using pressure relief measures, the proposed method had clearly positive effects on reliving pressure on the roof and floor of the roadway. The rates of change of roof subsidence, floor heave, internal movement of the left hand, and internal movement of the right hand were 23.33%, 23.85%, 32.93%, and 32.25%, respectively.

Comparing options 1 and 2, the pressure relief roadway was arranged on both sides of the roadway, which was beneficial for relieving pressure on the roof and floor of the roadway. It altered the rate of sinking of the roof by 25%. However, the effect of pressure relief on the two sides of the roadway was poor. Even after adopting the pres-

sure relief option, the deformation in the right hand was even larger. In addition, the installation of a pressure relief roadway on both sides of the roadway effectively controlled the sinking of the roof, and the rate of change in roof subsidence reached 25%, but the effect of pressure relief effect in the two sides of the roadway was not ideal.

A comparison of options 1 and 4 shows that the layout of the roadway determines the range of the pressure relief when the size of the pressure relief roadway is the same. The pressure relief roadway was arranged on each side of the mining roadway to help relieve pressure at the roof, and was arranged above the mining roadway, which helped pressure relief at the two sides of the roadway.

Comparing options 3 and 4 shows that when the position of the pressure relief roadway was selected consistently, the determination of lane size had a significant influence on the range of pressure relief. In option 3, by appropriately increasing the width of the pressure relief roadway, the deformation of the mining roadway was significantly reduced, and the rates of change of roof subsidence, floor heave, internal movement of the left hand, and internal movement of the right hand increased by more than 20%. The effect of pressure relief was thus prominent.

8. CONCLUSION

1) Selecting the position and size of the pressure relief roadway can significantly affect the stress distribution of rock surrounding the mining roadway. According to the calculation results of the FLAC 3D numerical simulation, selecting an appropriate roadway spacing and arranging the pressure relief roadway above or on both sides of the mining roadway can reduce stress due to rock surrounding the mining roadway. However, the low-pressure area formed by the pressure relief roadway above the mining roadway was larger than the low-pressure area formed by the pressure relief roadway on both sides of the mining roadway. In addition, within a certain range, appropriately increasing the width of the pressure relief roadway above the mining roadway effectively reduced stress in the surrounding rock and improved the environment of the mining roadway.
2) The excavation sequence of the pressure relief roadway and mining roadway had a significant influence on the effect of pressure. Following the excavation of the pressure relief roadway, once the stress variation in the surrounding rock had been stabilized, the mining roadway was excavated to significantly reduce or altogether avoid the disturbance caused by the excavation of the pressure relief roadway.
3) By comparing the effects of pressure relief of the four options, it was found that: the pressure relief roadway arranged on both sides of the mining roadway can best reduce the deformation of the roof. The pressure relief roadway was arranged directly above the mining roadway to effectively control the deformation

of the two sides of the mining roadway. Moreover, when the pressure relief roadway was arranged above the roof of the mining roadway, appropriately increasing the width of the roadway significantly improved the effect of pressure relief and controlled the malignant deformation of the surrounding rock.

ACKNOWLEDGEMENTS

The study was supported by Postgraduate Scientific Research Innovation Project of Hunan Province (grant numbers: CX20190794); The National Natural Science Foundation of China (grant numbers: 51874130; 51804109; 51774133; 51974118).

REFERENCES

GOU P.F., WANG C.B., ZHANG D.F., 2003, *Fuzzy comprehensive evaluation of the roadway support effect*, Ground Pressure and Strata Control, Vol. 20, No. 4, 4–5, 8.

GUO D.Y., HU J., WANG Y.K., 2017, *Coal and gas outburst level-extension warning technology and its application*, Chinese Journal of Safety Science, Vol. 27, No. 1, 88–92.

HAN C.L., ZHANG N., PEI J.G., YAN Z., 2017, *Mechanism and application of dual active control of "pressure relief-anchor" in retaining roadway along the go*, Journal of China Coal Society, Vol. 42, No. S2, 323–330.

HAN G., QI Q.J., CUI T.J., WANG L.G., 2018, *Research on risk assessment method and risk development trend of spontaneous combustion of residual coal*, Chinese Journal of Underground Space and Engineering, Vol. 14, No. 3, 852–858.

HOU C.J., 2017, *Research on key technology of surrounding rock control in deep roadway*, Journal of China University of Mining and Technology, Vol. 46, No. 5, 970–978.

LI J., MA N.J., DING Z.W., 2018, *Non-uniform large deformation mechanism and stability control of deep roadway along the direction of principal stress*, Journal of Mining and Safety Engineering, Vol. 35, No. 4, 670–676.

LI S.S., CUI T.J., MA Y.D., 2015, *Optimization of subway tunnel construction scheme based on cooperative game-cloud AHP*, China Safety Science and Technology, Vol. 11, No. 10, 156–161.

LI Z.M., WANG Y., 2018, *Plane numerical simulation analysis of the effect of pressure relief roadway*, Coal Engineering, Vol. 50, No. 3, 86–90, 94.

MA N.J., ZHAO X.D., ZHAO Z.Q., LI J., GUO X.F., 2015, *Analysis and control of roof stability in deep mining roadway*, Journal of China Coal Society, Vol. 40, No. 10, 2287–2295.

MA X.G., HE M.C., LI X.Z., WANG E.Y., HU C.W., GAO R., 2019, *Study on deformation mechanism and control countermeasures of overburden automatic roadway under overburden*, Journal of China University of Mining and Technology, Vol. 48, No. 3, 474–483.

MO S., TUTUK K., SAYDAM S., 2019, *Management of floor heave at Bulga Underground Operations–A case study*, International Journal of Mining Science and Technology, Vol. 29, No. 1, 73–78.

QIAN M.G., SHI P.W., ZOU X.Z. et al., 2003, *Mine pressure and rock formation control*, China University of Mining and Technology Press, Xuzhou.

WANG J.C., LU H.Y., WANG Z.H., ZHANG J.W., 2019, *Experimental study on the technical principle of fully mechanized caving mining in extra-thick coal seams*, Journal of China Coal Society, Vol. 44, No. 3, 906–914.

WANG M., WANG W., XIAO T.Q., 2017, *Decompression mechanism and key parameters determination method for deep mine roadway drilling*, Journal of China Coal Society, Vol. 42, No. 5, 1138–1145.

WANG W.J., YUAN C., YU W.J., WU H., PENG W.Q., PENG G., LIU X.S., DONG E.Y., 2016, *Study on the control method of surrounding rock stability in deep deformation roadway*, Journal of China Coal Society, Vol. 41, No. 12, 2921–2931.

XU H.J., ZHAO B.F., ZHOU Y., LIU S.Y., 2018, *Evaluation of water damage in the roof of working face based on entropy weight matter element extension model*, Journal of Mining and Safety Engineering, Vol. 35, No. 1, 112–117.

YU F.H., ZHAO T.B., TAN Y.L., GUO W.Y., 2016, *Discussion on quantitative calculation method of support strength of mining roadway under the influence of pressure relief mining*, Journal of Mining and Safety Engineering, Vol. 33, No. 3, 460–466.

ZHAO Z.Q., MA N.J., GUO X.F., ZHAO X.D., FAN L., 2016, *Mechanism and control of butterfly blade roofing in large deformation mining roadway*, Journal of China Coal Society, Vol.41, No. 12, 2932–2939.

ZHANG K.X., BAI J.B., HAO Y.X., LI L., ZHANG Y.J., WANG W., XU L., PAN Y.W., 2010, *Multi-level fuzzy comprehensive evaluation of bolting effect of coal roadway*, Coal Science and Technology, Vol. 38, No. 8, 10–14.

ZHANG M.L., ZHANG Y.D., JI M., CHENG L., HUANG W., 2016, *Optimization of roadway support parameters based on fuzzy extension comprehensive evaluation method*, Journal of Mining and Safety Engineering, Vol. 33, No. 6, 972–978.

ZHU W.C., HOU C., LIU X.G., ZHANG M.S., 2015, *Numerical analysis of pressure relief of surrounding rock by two horizontal groovings in circular roadway*, Chinese Journal of Underground Space and Engineering, Vol. 11, No. 6, 1462–1469.

ZUO J.P., SHI Y., LIU D.J., SUN Y.J., CHEN Y., 2019, *Equivalent ellipse model and simulation analysis of slotting and pressure relief in deep soft rock roadway*, Journal of China University of Mining and Technology, Vol. 48, No. 1, 1–11.